Supplementary Information

A Solid-state NMR Method for Structure Solution of Zeolite Crystal Structures

*Darren H. Brouwer,[†] Richard J. Darton,[‡] Russell E. Morris,[‡] and Malcolm H. Levitt[†,]**

[†]School of Chemistry, University of Southampton, Southampton, SO17 1BJ, UK and [‡]School of Chemistry, University of St. Andrews, St. Andrews, KY16 9ST, UK

OUTLINE

1. Solid-state NMR pulse sequence

The pulse sequence diagram of the solid-state NMR experiment used to probe the internuclear distances between ^{29}Si – ^{29}Si spin pairs in pure silica zeolite frameworks is displayed in Figure S1. The experiment employs the symmetry-based homonuclear dipolar recoupling sequence SR26$_4^{11}$ to excite and reconvert double-quantum (DQ) coherences between dipolar coupled ^{29}Si nuclei.[1]

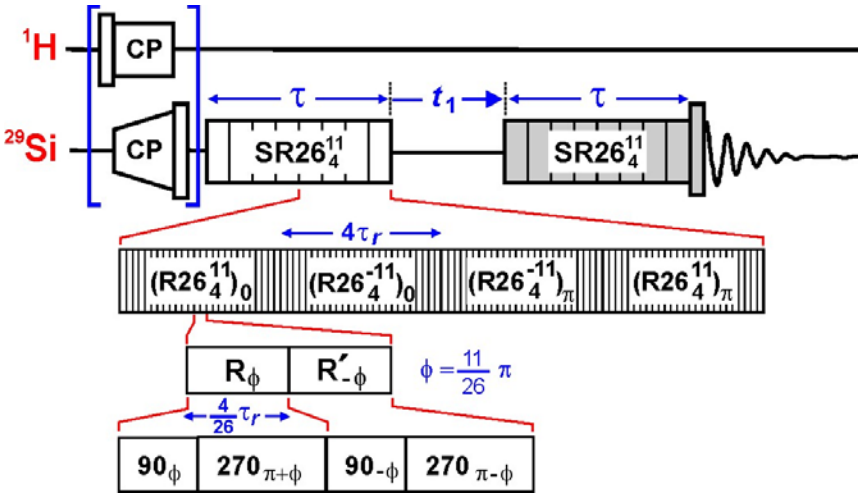

Figure S1. Pulse sequence diagram for two-dimensional ^{29}Si double-quantum correlation spectroscopy using the SR26$_4^{11}$ dipolar recoupling sequence.

The SR26$_4^{11}$ dipolar recoupling sequence[2] is a supercycled version of a RN_n^{ν} sequence[3] and is of the form

$$SRN_n^{\nu} = (RN_n^{\nu})_0\,(RN_n^{-\nu})_0\,(RN_n^{-\nu})_\pi\,(RN_n^{\nu})_\pi$$

with $N = 26$, $n = 4$, and $\nu = 11$. RN_n^{ν} denotes the symmetry-based pulse sequence given by

$$RN_n^{\nu} = [R_\phi\, R'_{-\phi}]^{N/2}$$

where R is a composite π pulse that rotates the spins by $\pm\pi$ about the *x*-axis and R′ is derived from R by changing the signs of all phases. The subscript ϕ denotes the overall r.f. phase shifts of the R elements and is given by

$$\phi = \pi\,\nu/N$$

while the superscript $N/2$ denotes the number of repetitions of the bracketed elements. In the present case, the R element is the composite π pulse

$$R = R' = (\pi/2)_0(3\pi/2)_\pi.$$

The r.f. field strength is set so that one RN_n^ν sequence occupies exactly *n* rotor periods. With this particular R element, the r.f. field strength must be set to exactly N/n times the spinning frequency. The $SR26_4^{11}$ sequence can be written explicitly as

$$[90_{76.15}\,270_{256.15}\,90_{283.85}\,270_{103.85}]^{13}\,[90_{283.85}\,270_{103.85}\,90_{76.15}\,270_{256.15}]^{13}$$

$$[90_{103.85}\,270_{283.85}\,90_{256.15}\,270_{76.15}]^{13}\,[90_{256.15}\,270_{76.15}\,90_{103.85}\,270_{283.85}]^{13}$$

where the subscripts are the phases of the pulses (in degrees) while the superscripts denote 13 repetitions of the bracketed elements. One complete supercycle spans 16 rotor periods and requires an r.f. field strength that provides a nutation frequency which is exactly 6.5 times the spinning frequency.

The $SR26_4^{11}$ recoupling sequence is incorporated into a 2D DQ correlation experiment as follows. If $^1H\rightarrow{}^{29}Si$ cross polarization is employed, a 90° pulse is applied after ramped cross polarization to generate longitudinal magnetization. A $SR26_4^{11}$ recoupling sequence of duration τ excites DQ coherences which are then allowed to evolve during t_1 and are consequently reconverted into longitudinal magnetization by a second $SR26_4^{11}$ recoupling sequence of the same duration τ. The shaded elements are given a four-step phase cycle to select signals passing through DQ coherences. Pure absorption 2D spectra are obtained by using the TPPI method in which all of the pulses prior to

the t_1 evolution period are given phase shifts in increments of 45° as t_1 is incremented and a cosine Fourier transform is applied in the indirect dimension.

2. Calculation of double-quantum curves

2.1 Double-quantum curves for two-spin systems

The DQ signal intensity as a function of the recoupling time τ (the DQ curve) with the $SR26_4^{11}$ dipolar recoupling sequence for a pair of coupled spins-1/2 may be estimated using the first-order average Hamiltonian symmetry theory.[4] The result is

$$S(\alpha_{PR},\beta_{PR},\gamma_{PR};b_{ij},\tau)=\sin^2\left(\frac{3}{2}|\kappa|b_{ij}\tau\sin 2\beta_{PR}\cos\gamma_{PR}\right) \qquad \text{(S1)}$$

where the Euler angles describing the orientation of the internuclear vector with respect to the rotor axis are $\{\alpha_{PR},\beta_{PR},\gamma_{PR}\}$ and b_{ij} is the homonuclear dipolar coupling constant (in rad s^{-1}) between spins i and j and is proportional to the inverse cube of the internuclear distance r_{ij}:

$$b_{ij}=-\frac{\mu_0}{4\pi}\hbar\frac{1}{r_{ij}^3}\gamma^2 \qquad \text{(S2)}$$

κ is the complex scaling factor of the dipolar interaction and has a magnitude given by $|\kappa| = 0.1708$ for $R26_4^{11}$ symmetry, according to the equations in ref. 5. To calculate the DQ curve for a powder, equation S1 must be integrated over all crystallite orientations:

$$S(b_{ij},\tau)=\frac{1}{4\pi}\int_0^{2\pi}\mathrm{d}\gamma_{PR}\int_0^{\pi}\sin\beta_{PR}\,\mathrm{d}\beta_{PR}\sin^2\left(\frac{3}{2}|\kappa|b_{ij}\tau\sin 2\beta_{PR}\cos\gamma_{PR}\right) \qquad \text{(S3)}$$

Since the structure solution algorithm must calculate large number of DQ curves, it is of paramount importance that the expression for the DQ curves can be evaluated very quickly. Fortunately, this

integral can be expressed in the same form as the equation for the REDOR curve[6] which Mueller et al. have shown may be simplified in terms of quarter-order Bessel functions of the first kind:[7,8]

$$S(b_{ij},\tau) = \frac{1}{2} - \frac{\sqrt{2}\pi}{8} J_{1/4}\left(\frac{3}{2}|\kappa|b_{ij}\tau\right) J_{-1/4}\left(\frac{3}{2}|\kappa|b_{ij}\tau\right) \qquad \text{(S4)}$$

A set of DQ curves, calculated with this expression, for a range of Si – Si distances expected in zeolite frameworks is displayed in Figure S2a. The above equations are only valid in the first order of average Hamiltonian theory. We have checked the validity of this approximation by performing accurate spin dynamical simulations for 2-spin-1/2 systems, using dipole-dipole coupling and chemical shift anisotropy parameters appropriate for ^{29}Si sites in zeolites. The deviations from the analytical formula (S4) were found to be negligible in all cases of interest, as shown in Figure S2b.

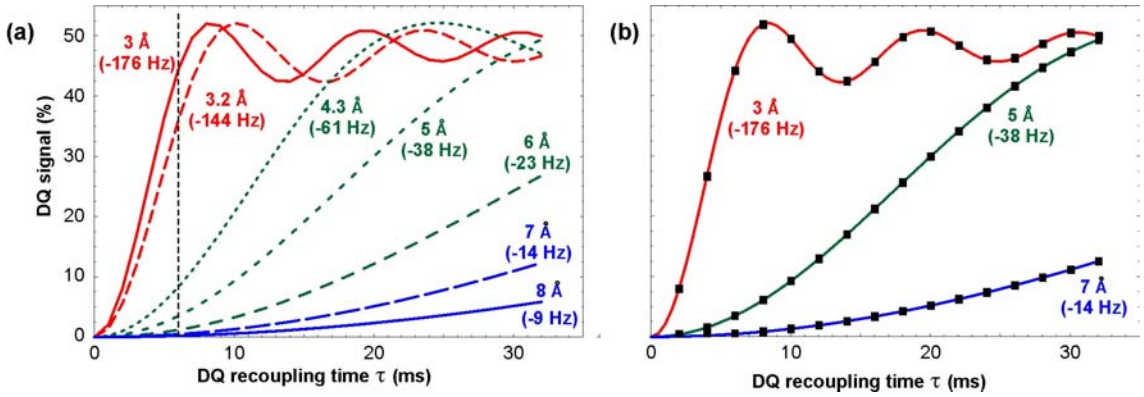

Figure S2. Double quantum curves for isolated ^{29}Si-^{29}Si spin pairs for the SR26$_4$[11] dipolar recoupling experiment. (a) Calculated DQ curves for using the analytical function in equation S4 for various distances and corresponding dipolar couplings expected for ^{29}Si-^{29}Si spin pairs in zeolites. The vertical dashed line indicates a recoupling time of 6 ms at which the spin pairs across Si-O-Si bonds can be clearly distinguished from the longer range interactions. (b) Comparison of the DQ curves calculated using the analytical function in equation S4 (solid lines) to SIMPSON[9] simulations (black squares) using typical ^{29}Si chemical shift parameters for purely siliceous zeolites: $\Delta\delta_{1,2}^{iso}$ = 7.3 ppm, δ_1^{aniso} = 10.4 ppm, η_1 = 0.6, δ_2^{aniso} = 10.4 ppm, η_2 = 0.4, $\omega_r/2\pi$ = 4 kHz. The simulated DQ curves were averaged over18450 crystallite orientation.

2.2 Full double-quantum curves

The full DQ curves for each pair of Si sites *i* and *j*, denoted as $S_{ij}(\tau)$, were calculated as follows. The fractional coordinates of Si sites *i* and *j* in the asymmetric unit of the crystal structure are denoted as $\vec{r}_i$ and $\vec{r}_j$ respectively. A set of distinct symmetry-related positions of Si site *j* were generated from $\vec{r}_j$ using $\vec{r}_j^{(s)} = \mathbf{O}^{(s)}\vec{r}_j$ where $\mathbf{O}^{(s)}$ denotes one of s = 1 .. N_{sym} space group symmetry operators which map positions in the asymmetric unit to symmetry-related positions in neighbouring units. The distance $r_{ij}^{(s)}$ between atoms at positions $\vec{r}_i$ and $\vec{r}_j^{(s)}$ was calculated by $r_{ij}^{(s)} = \left|\mathbf{M}\left(\vec{r}_i - \vec{r}_j^{(s)}\right)\right|$ where $\mathbf{M}$ is the metric matrix which converts fractional coordinates into Cartesian coordinates. The DQ curve for the

spin pair with atoms at positions $\vec{r}_i$ and $\vec{r}_j^{(s)}$, separated by the distance $r_{ij}^{(s)}$, was calculated according to

$$S_{ij}^{(s)}(\tau) = \begin{cases} 0 & \text{if } r_{ij}^{(s)} > r_{\max} \\ 1/2 - \left(\sqrt{2}\pi/8\right) J_{1/4}\left(\tfrac{3}{2}|\kappa| b_{ij}^{(s)}\tau\right) J_{-1/4}\left(\tfrac{3}{2}|\kappa| b_{ij}^{(s)}\tau\right) & \text{if } r_{ij}^{(s)} \le r_{\max} \end{cases} \qquad \text{(S5)}$$

where $r_{\max}$ is the cut-off distance ($r_{\max}$ = 8 Å in these calculations) and $b_{ij}^{(s)}$ is the dipolar coupling constant corresponding to the distance $r_{ij}^{(s)}$ (calculated with equation S2). The full DQ curve for the pair of Si sites *i* and *j* was constructed by summing the curves for each of the spin pairs:

$$S_{ij}(\tau) = A \exp\{-k\tau\} \; (p_i \, p_j) \sum_{s=1}^{N_{sym}} S_{ij}^{(s)}(\tau) \qquad \text{(S6)}$$

where p_i and p_j are the relative site occupancies of Si sites *i* and *j* respectively and the function $A \exp\{-k\tau\}$ is applied in order to scale the data and account for relaxation. Note that the parameters *A* and *k* are not specific for a particular pair of Si sites; the same values of *A* and *k* were used for every DQ curve.

It is important to note that, due to the natural abundance of ^{29}Si (4.7%), it is valid to sum the DQ curves of ^{29}Si-^{29}Si spin pairs and ignore the more complex curves that would arise from clusters of three or more ^{29}Si nuclei.

3. Structure solution algorithm

3.1 Definition of least-squares minimum

The goal is to determine the fractional coordinates of the Si sites in the asymmetric unit which minimize the sum of the squares of the residuals between the experimental and calculated DQ curves:

$$\chi^2_{\mathrm{DQ}}(A,k;\vec{r}_1,\vec{r}_2,...,\vec{r}_{N_{Si}}) = \sum_{i=1}^{N_{\mathrm{Si}}}\sum_{j=1}^{i}\sum_{l=1}^{N_\tau} w_{ijl}\left\{S_{ij}^{\mathrm{obs}}(\tau_l) - S_{ij}^{\mathrm{calc}}(\tau_l)\right\}^2 \qquad \text{(S7)}$$

S^{obs} is the set of experimental DQ curves. S^{calc} is the set of calculated DQ curves which are functions of the fractional coordinates $\vec{r}_i$ of Si atoms $i = 1, 2, \ldots, N_{\mathrm{Si}}$, the scaling factor A and the damping factor k. The elements of these sets, denoted by $S_{ij}^{\mathrm{obs}}(\tau_l)$ and $S_{ij}^{\mathrm{calc}}(\tau_l)$ represent the respective values for the lth recoupling time point ($l = 1, 2, ..., N_\tau$) of the DQ curve for the correlation involving Si site i and Si site j. $S_{ij}^{\mathrm{calc}}(\tau_l)$ is calculated from $\vec{r}_i$, $\vec{r}_j$, A, and k according to equation S6 as described in the previous section. w_{ijl} is the weight for the lth data point in the DQ curve for Si sites i and j and is set to $w_{ijl} = 1/\sigma_{ijl}^2$ where σ_{ijl} is the estimated error of the ijlth experimental data point.

In order to facilitate comparisons between different sets of experimental data, the quality of fit of the structure to the experimental solid-state NMR data is defined as:

$$R_{\mathrm{DQ}} = \sqrt{\frac{\sum_{i=1}^{N_{\mathrm{Si}}}\sum_{j=1}^{i}\sum_{l=1}^{N_\tau} w_{ijl}\left\{S_{ij}^{\mathrm{obs}}(\tau_l) - S_{ij}^{\mathrm{calc}}(\tau_l)\right\}^2}{\sum_{i=1}^{N_{\mathrm{Si}}}\sum_{j=1}^{i}\sum_{l=1}^{N_\tau} w_{ijl}\left\{S_{ij}^{\mathrm{obs}}(\tau_l)\right\}^2}} \qquad \text{(S8)}$$

3.2 Grid Search

In order to ensure that the global minimum of χ^2_{DQ} is found, the fractional coordinate space must be sampled thoroughly. In this section, an efficient grid search is described which yields a set of "grid structures" of the Si sites that are close to the minimum χ^2_{DQ}. These grid structures can be used as initial values of the fractional coordinates in a non-linear least squares minimization of χ^2_{DQ}. This combination of grid search and subsequent minimization should ensure that the global minimum of χ^2_{DQ} is found.

The grid search consists of building up candidate structures one Si site at a time with the atomic coordinates restricted to points on a three-dimensional grid of the asymmetric unit. The first step is to define a three-dimensional grid of the asymmetric unit. We have found that a resolution of about 0.5 to 0.75 Å between grid points in all three crystallographic directions is a good balance between the time required to perform the calculations and fully sampling the coordinate space. The maximum distance between two grid points is defined as

$$\Delta_{grid} = (\Delta a^2 + \Delta b^2 + \Delta c^2)^{1/2}$$

where Δa, Δb, and Δc are the distances between adjacent grid points along the *a*, *b*, and *c* crystallographic axes respectively.

G_n denotes the set of candidate grid structures in which each structure consists of *n* Si sites. To construct G_n, the possible grid positions for the *n*th Si site to be incorporated into the structures are added to each of the G_{n-1} candidate grid structures and the relative occupancies, inter-site connectivities, and quality of fit to the experimental DQ curves are evaluated, as described in the following.

The possible grid positions for the added Si site are limited to those for which the connectivity between symmetry-related positions of the same Si site is satisfied. For example, the intensity of the

"auto-correlation" in the 2D ^{29}Si DQ correlation spectrum of test sample **1** (Figure 3b) indicates that site D is connected to two symmetry-related positions of site D. In this case, the possible grid points for site D are limited to those grid points for which the two closest positions of site D in adjacent asymmetric units generated by symmetry both have distances from the grid point in the interval [3.0 Å - Δ_{grid}, 3.2 Å + Δ_{grid}]. The distance between Si atoms across Si-O-Si linkages are known to be between 3.0 and 3.2 Å. The Δ_{grid} term accounts for the fact that the atomic positions are strictly limited to the grid points while the actual atomic positions may fall somewhere between the grid points. Additionally, there should be no distances between the grid point and its symmetry equivalents that are less than 3.0 Å - Δ_{grid} as these short distances are physically unreasonable for pure silica zeolites. Furthermore, all of the other symmetry equivalent positions must be at least two Si-O-Si linkages apart which corresponds to these distances being greater than 4.3 Å - Δ_{grid} as 4.3 Å is the minimum distance for Si atoms across two Si-O-Si bonds.

The grid positions which satisfy the "self-connectivity" for the added Si site are incorporated into each of the candidate structures in the set G_{n-1} to give the set of new candidate grid structures G_n'.

Each of the new candidate grid structures in the set G_n' is then evaluated to ensure that the relative occupancies of the sites are consistent with the relative intensities in the 1D ^{29}Si MAS NMR spectrum.

For those grid structures with the correct site occupancies, the connectivities between the Si sites are evaluated to ensure that they are in agreement with the connectivity matrix derived from the 2D ^{29}Si DQ correlation spectrum acquired with a short DQ recoupling time. As with the evaluation of the "self-connectivities", the inter-site connectivities in the candidate grid structures are deemed to be correct if the set of distances between the grid position for Si site *i* in the asymmetric unit and the symmetry-related grid positions for Si site *j* (including the grid position of site *j* in the asymmetric unit) meet the following criteria: (1) there are no distances less than 3.0 - Δ_{grid}, (2) there are at least c_{ij} distances in the interval [3.0 Å - Δ_{grid}, 3.2 Å + Δ_{grid}] where c_{ij} denotes the *ij*th element of the connectivity matrix

derived from the 2D NMR spectrum, and (3) With the exception of the first c_{ij} distances, all other distances are greater than 4.3 - Δ_{grid}.

For those grid structures with meet the connectivity criteria, the quality of fits to the relevant experimental DQ curves are then evaluated. The DQ curves for those Si sites that have been incorporated into the grid structures are calculated from the distances between the grid positions according to equation S6 as described earlier. For each grid structure, A and k are adjusted in order to minimize χ^2_{DQ}. The grid structures are then sorted according to their R_{DQ} values and a set of the best grid structures with $R_{DQ} < c_{select}\,(R_{DQ})_{min}$ are selected where $(R_{DQ})_{min}$ denotes the R_{DQ} value of the grid structure which best agrees with the experimental DQ curves and c_{select} is a user-defined constant (usually between 1.1 and 2.0).

This set of grid structures is denoted G_n. The next Si site is added to each of these grid structures and the whole process described above is repeated until all of the Si sites have been incorporated. The final set of grid structures should be close to the global minimum in χ^2_{DQ}. The global minimum should be found by using the fractional coordinates in each of the grid structures as the initial values in a local non-linear least-squares minimization of χ^2_{DQ}.

3.3 Least-squares minimization

For the least-square minimization of the final grid structures, the cost function was modified to include restraints on the Si – Si distances between Si atoms known to share a Si-O-Si linakge:

$$\chi^2_{DQ,r} = \chi^2_{DQ} + w_r \sum_{i=1}^{N_{Si}} \sum_{j=1}^{i} \sum_{m=1}^{c_{ij}} \{r_{ijm} - r_0\}^2 \qquad \text{(S8)}$$

r_{ijm} represents the mth closest distance between the position of Si site i ($\vec{r}_i$) in the asymmetric unit and the set of symmetry-related positions of Si site j ($\vec{r}_j^{(s)}$) where $m = 1$ .. c_{ij} and c_{ij} is the ijth element of the

connectivity matrix, representing the number of Si-O-Si linkages between Si site *i* and the symmetry related positions of Si site *j*. The target distance is represented by r_0 and is set to 3.1 Å in these calculations as the Si – Si distances across Si-O-Si linkages are known to fall within the narrow range of about 3.0 to 3.2 Å. The weight factor w_r was adjusted so that the average deviation of the restrained distances from the target distance in the minimized structure was approximately 0.05 Å. The least-squares minimization was carried out using the Gauss-Newton method as described by Nocedal and Wright[10].

3.4 Structure completion and distance least-squares

The structure solution algorithm provides the atomic coordinates for the Si sites, which is sufficient to define the zeolite framework structure. In order to provide a complete structure for refinement against the powder XRD pattern, oxygen atoms can be added midway between Si sites which share Si-O-Si linkages.

Once the oxygen atoms are added, it is possible to optimize the geometry of the zeolite framework using the Distance Least-Squares (DLS) procedure[11] in which the Si-O, O-O, and Si-Si distances are optimized by minimizing the sum of the squares of the residuals between calculated and prescribed interatomic distances:

$$\chi^2_{\mathrm{DLS}} = \sum_{j,m,n} w_j \left\{ r_j^{m,n} - r_j^0 \right\}^2$$

in which r_j^0 is the prescribed interatomic distance of type *j*, $r_j^{m,n}$ is the calculated interatomic distance of type *j* between atoms *m* and *n*, and w_j is the weight ascribed to interatomic distances of type *j*. In order to compare the results of DLS optimization on different structures, the following parameter was defined

$$R_{\mathrm{DQ}} = \sqrt{\frac{\sum_{j,m,n} w_j \left\{ r_j^{m,n} - r_j^0 \right\}^2}{\sum_{j,m,n} w_j \left\{ r_j^0 \right\}^2}}$$

For the DLS optimizations performed here, the prescribed distances were $r^0_{\mathrm{Si-O}} = 1.61$, $r^0_{\mathrm{O-O}} = 2.629$,and $r^0_{\mathrm{Si-Si}} = 3.07$ and the weight values were $w_{\mathrm{Si-O}} = 2.0$, $w_{\mathrm{O-O}} = 0.61$, and $w_{\mathrm{Si-Si}} = 0.23$. These distances and weight values were used to generate the idealized frameworks reported in the *Atlas of Zeolite Structure Types.*[12] The unit cell parameters remained fixed.

4. Structure determination of zeolite test sample 1

4.1 Synthesis

Test sample **1** (pure silica zeolite ITQ-4) was synthesized and then calcined to remove the organic template molecules as described in the literature.[13] The synthesis and calcination was carried out by the group at the University of St. Andrews.

4.2 Powder XRD

Powder XRD data (7 – 75 $^{\mathrm{o}}$ 2θ) were collected in transmission mode on a Stoe STADIP diffractometer equipped with a monochromator (Cu Kα, λ = 1.54056 Å) and a position sensitive detector. The powder diffraction pattern was indexed with the TREOR program[14] to give the unit cell parameters *a*=18.669 *b*=13.503, *c*=7.662 Å, β=102.1° and the monoclinic space group *I* 2/*m*. The sample was then sent for solid-state NMR analysis at the University of Southampton.

4.3 Solid-state NMR

The quantitative 1D ^{29}Si MAS NMR spectrum of zeolite test sample **1** is presented in Figure 3a. This spectrum was obtained at a spinning frequency of 4000 Hz with 128 acquisitions, each with a 45°

pulse and 60 s recycle delay. The spectrum was fit with four Lorentzian peaks of equal area as shown in Figure 3a and summarized in Table S1. The ^{29}Si T_1 relaxation times were measured with a saturation recovery sequence and these values are listed in Table S1.

The complete series of 2D ^{29}Si DQ correlation spectra acquired at various recoupling times (obtained with the $SR26_4^{11}$ pulse sequence described in Figure S1) is presented in Figure S5. The spinning frequency was 4000 Hz and the ^{29}Si nutation frequency during recoupling was 26.5 kHz. Each 2D experiment consisted of 40 t_1 increments each with 100 acquisitions with the exception of the experiments with recoupling times of 4 and 6 ms in which the number of acquisitions were 180 and 128 respectively. t_1 was incremented in steps of 250 μs (i.e. exactly one rotor period). The recycle delay was 10 s after presaturation pulses were applied. Exponential line broadening of 10 and 20 Hz was applied in the single-quantum and double-quantum dimensions respectively.

The inter-site connectivities (see Table S2) were established by evaluating the relative intensities of the correlations in the 2D DQ correlation spectrum with a recoupling time of 6 ms. The amplitudes of the correlation peaks were extracted from the 2D spectra to give the DQ curves presented in Figure 4. The DQ intensities were scaled with respect to the peak intensities in a 1D ^{29}Si MAS spectrum acquired with the same recycle delay of 10 s after presaturation pulses.

Table S1. NMR parameters for zeolite test sample **1**.

Peak	Chemical Shift[a] (ppm)	Relative Peak Area[a]	Peak Width at Half Height[a] (Hz)	% Lorentzian[a]	T_1[b] (s)	Correlated Peaks[c]
A	-107.7	1	21	100	5.3	B,B,C,D
B	-109.4	1	21	100	4.9	A,A,B,C
C	-110.6	1	25	100	6.2	A,B,C,D
D	-112.3	1	12	100	9.6	A,C,D,D

[a] Obtained from deconvolution of 1D ^{29}Si MAS NMR spectrum (Figure 3a). [b] Measured with a saturation recovery experiment. [c]Determined from the 2D ^{29}Si DQ correlation spectrum obtained with a recoupling time of 6 ms (Figure 4)

Table S2. Inter-site connectivity matrix* for zeolite test sample **1**.

	A	**B**	**C**	**D**
A	0	2	1	1
B	2	1	1	0
C	1	1	1	1
D	1	0	1	2

* The number in row *i* and column *j* indicates the number of Si sites *j* that are connected via Si-O-Si linkages to Si site *i.* Derived from the relative intensities of the correlation peaks in the 2D DQ correlation spectrum obtained with a recoupling time of 6 ms.

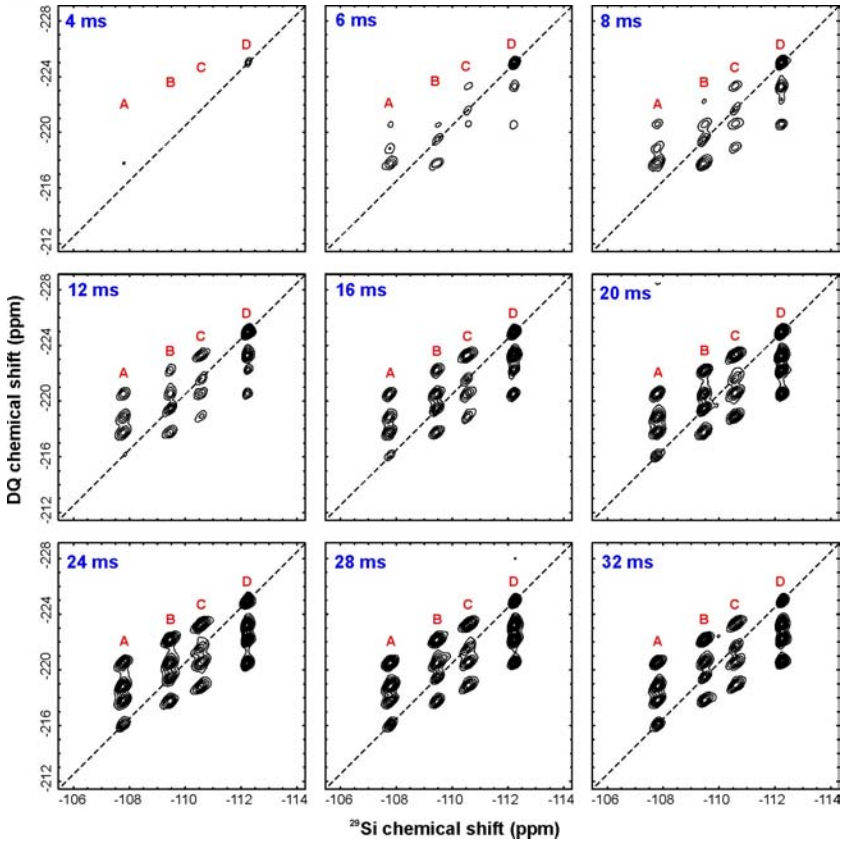

Figure S5. Two-dimensional ^{29}Si SR26$_4^{11}$ double-quantum correlation spectra of zeolite test sample **1** obtained at the indicated recoupling times.

4.4 Structure solution by solid-state NMR

The asymmetric unit for the *I* 2/*m* space group was chosen to be $0 \leq x \leq 1/2$, $0 \leq y \leq 1/4$, $0 \leq z < 1$. A three dimensional grid of the asymmetric unit was defined with a resolution of approximately 0.5 Å such that there were 20, 8, and 15 grid points in the *a*, *b*, and *c* directions respectively. After evaluating the "self-connectivity" information which limited the possible grid positions for sites A, B, C, and D to 847, 1010, 1010, and 226 positions respectively, the order in which the sites were added was set to {D, A, B, C}. Furthermore, the grid positions for the first site were limited to those positions for which $0 \leq z \leq 1/4$ in order to cut down on the number of identical solutions which arise due to a number of equivalent choices of the origin. The number of grid structures

at each stage of the grid search are presented in Table S3. The grid search required 30 minutes of computation time.

Table S3. Summary of grid search for zeolite test sample **1**.

n	Added Si site	Possible positions for added Si site	New candidate structures	Consistent with relative occupancies	Consistent with inter-site connectivities	c_{select}	Best agreement with DQ curves*
1	D	58	58	58	58	2.0	21
2	A	847	17 787	13 230	4 080	1.4	218
3	B	1 010	219 919	202 479	3 894	1.3	356
4	C	1 010	358 828	330 348	6 009	1.1	58

* Candidate structures with $R_{DQ} < c_{select}(R_{DQ})_{min}$ were selected

The 58 best grid structures were then subjected to non-linear least-squares minimization with the Si – Si distances across Si-O-Si linkages restrained to 3.10 ± 0.05 Å by setting $w_r = 0.15$. These minimized structures were compared to each other and 10 unique structures were identified. Oxygen atoms were added to each structure and the structures were subjected to DLS optimization in order to test the geometric feasibility of the structures. Additionally, the structures were evaluated for the presence of "three-rings" which are highly unlikely to be found in the structure, given the ^{29}Si chemical shifts observed. Table S4 lists the unique minimized structures, sorted according to the R_{DQ} values, along with the R_{DLS} values and whether or not there exist three-rings in the structure.

Table S4. Unique minimized structures determined by solid-state NMR

Structure	R_{DQ}	R_{DLS}	Three-rings?
1	0.1043	0.0400	yes
2	**0.1043**	**0.0035**	**no**
3	0.1062	0.0522	yes
4	0.1062	0.0520	yes
5	0.1080	0.0609	yes
6	0.1081	0.0320	yes
7	0.1086	0.0755	yes
8	0.1087	0.0755	yes
9	0.1173	0.0296	yes
10	0.1189	0.0656	yes

It is very clear that structure 2 in this table is the most likely structure for zeolite test sample **1** as it gives one of lowest R_{DQ} values and all of the other structures give R_{DLS} values that are an order of magnitude greater due to the presence of unfavourable three-rings. This "solid-state NMR structure" is presented in Figure 3 and the set of Si – Si distances calculated from this structure was used to calculate the DQ curves presented in Figure 2c (with $A = 1.86$ and $k = 28.4\ s^{-1}$). This structure solved by solid-state NMR is compared to the XRD-refined structure in Figure 3b. The atomic coordinates for the Si sites determined by solid state are listed and compared to the refined coordinates in Table S6. The absolute differences in the atomic coordinates between the solid-state NMR and XRD-refined structure are all less than 0.5 Å.

4.5 Structure completion and refinement against powder XRD data

Structure refinement of test sample **1** was carried out using the whole pattern fitting (Rietveld) method incorporated into the GSAS suite of programs.[15] The four silicon atoms from the NMR structure solution were used as the starting model, and the remaining oxygen atoms were found from subsequent difference Fourier syntheses. The initial stages of the refinement included restraints (soft constraints) to ensure chemically sensible geometries in the model, but these were removed towards the end of the refinement. The final cycle of least squares refinement included terms for the atomic positions of all the atoms, together with two variables for the silicon and oxygen isotropic displacement parameters respectively. The final refinement cycle also included terms for the lattice parameters, diffractometers zero point and profile (peak shape and background). The refinement converged to values of $R_p = 0.0558$, $wR_p = 0.0745$ and $\chi^2 = 4.48$. The observed, calculated and difference profiles for the refinement are shown in Figure S6. The final refined unit cell parameters and atomic coordinates are listed in Table S5.

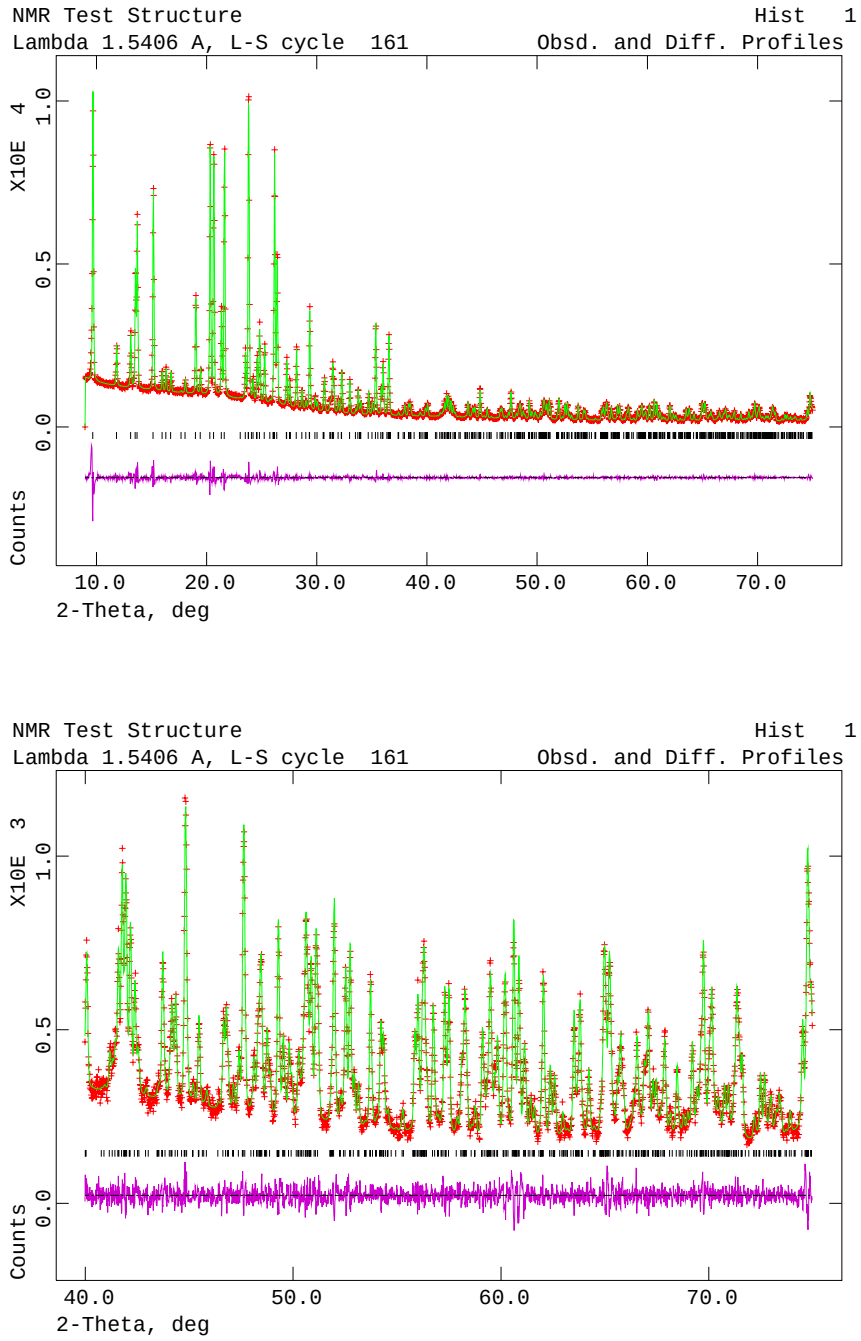

Figure S6. Rietveld refinement plots for zeolite test sample **1**. The observed (red crosses), calculated (green line) and difference (purple) plots for the Rietveld refinement of the structure against powder X-ray diffraction data. The high angle portion of the plot is enlarged to show the quality of the fit in this region more clearly.

Table S5. Final unit cell, refined coordinates and isotropic displacement parameters for zeolite test sample **1**.

Unit cell: a = 18.66363(24) Å b = 13.49929(16) c = 7.63419(10) Beta = 101.9910(10) Cell volume = 1881.43(4) $Å^3$

Atom	x	y	z	Uiso
Si1	0.16027(19)	0.20495(28)	0.3864(5)	0.0225(5)
Si2	0.25013(20)	0.11133(29)	0.1242(5)	0.0225(5)
Si3	0.14442(19)	0.11292(27)	0.7454(5)	0.0225(5)
Si4	0.01395(20)	0.10921(31)	0.2151(4)	0.0225(5)
O1	0.32077(36)	0.1830(5)	0.1408(10)	0.0245(10)
O2	0.20775(38)	0.1307(5)	0.2884(10)	0.0245(10)
O3	0.17795(34)	0.1789(5)	0.6042(10)	0.0245(10)
O4	0.07325(39)	0.1879(5)	0.3019(10)	0.0245(10)
O5	0.27342(51)	0.000000	0.1300(14)	0.0245(10)
O6	0.19098(38)	0.1404(5)	0.9434(10)	0.0245(10)
O7	0.15492(48)	0.000000	0.7038(12)	0.0245(10)
O8	0.05906(41)	0.1382(5)	0.7340(9)	0.0245(10)
O9	0.000000	0.1253(8)	0.000000	0.0245(10)
O10	0.03464(49)	0.000000	0.2578(14)	0.0245(10)

Table S6. Comparison of Si fractional atomic coordinates for zeolite test sample **1** determined by solid-state NMR and subsequent refinement against powder XRD data.

Si site		Solid-state NMR	Powder XRD	Difference (Å)
A	*x*	0.1735	0.1603	0.48
	y	0.1861	0.2049	
	z	0.4354	0.3864	
B	*x*	0.2562	0.2501	0.25
	y	0.1149	0.1113	
	z	0.1562	0.1242	
C	*x*	0.1455	0.1444	0.38
	y	0.1152	0.1129	
	z	0.7949	0.7454	
D	*x*	0.0249	0.0140	0.27
	y	0.1183	0.1092	
	z	0.2039	0.2151	

4.6 Structure solution from powder XRD

Initial attempts to solve the structure of zeolite test sample **1** using individual reflection intensities extracted using the Le Bail method (GSAS) followed by use of a single crystal direct methods structure solution program (SIR 97) were unsuccessful. Subsequently, the program EXPO[16] was used to extract reflection intensities and solve the structure using the direct methods algorithm specially designed to take into account the reflection overlap difficulties encountered in powder X-ray diffraction. All four of the crystallographically independent silicon atoms, plus several potential oxygen positions were thus located.

5. Structure determination of zeolite test sample 2

5.1 Synthesis

Test sample **2** (pure silica zeolite ferrierite) was synthesized as described in the literature.[17,18] The synthesis was carried out by the group at the University of St. Andrews. The sample was used in its as-synthesized form, with the template molecules remaining within the zeolite channel system.

5.2 Powder XRD

Powder XRD data (7 – 75 ^{o} 2θ) were collected in transmission mode on a Stoe STADIP diffractometer equipped with a monochromator (Cu Kα, λ = 1.54056 Å) and a position sensitive detector. The powder diffraction pattern was indexed with the Treor program to give the unit cell parameters *a*=7.4068, *b*=14.0713, *c*=18.6699 Å and the orthorhombic space group *Pnnm*. The sample was then sent for solid-state NMR analysis at the University of Southampton.

5.3 Solid-state NMR

Since the organic template molecules still reside within the zeolite framework, $^{1}H \rightarrow ^{29}Si$ cross polarization (CP) was found give a substantial gain in signal over direct ^{29}Si polarization for this sample. The 1D ^{29}Si CP MAS NMR spectrum of zeolite test sample **2** is presented in Figure S7. This spectrum was obtained at a spinning frequency of 4000 Hz with 64 acquisitions, each with a 40 ms contact time and 2.5 s recycle delay after presaturation pulses were applied on the ^{1}H channel. The ^{1}H T_1 relaxation time was measured to be approximately 2 s. The spectrum was fit with five peaks with relative intensities 2:2:2:2:1 as shown in Figure S7 and summarized in Table S7.

The complete series of 2D ^{29}Si DQ correlation spectra acquired at various recoupling times (obtained with the $SR26_4^{11}$ pulse sequence described in Figure S1) is presented in Figure S8. The spinning frequency was 4000 Hz and the ^{29}Si nutation frequency during recoupling was 26.5 kHz. Each 2D experiment consisted of 40 t_1 increments each with 240 or 320 acquisitions with the exception of the experiments with a recoupling times of 6 ms in which the number of acquisitions was 600. t_1 was

incremented in steps of 250 μs (i.e. exactly one rotor period). The contact time was 40 ms and the recycle delay was 2.5 s. Exponential line broadening was not applied in either dimension.

The inter-site connectivities (see Table S8) were established by evaluating the relative intensities of the correlations in the 2D DQ correlation spectrum with a recoupling time of 6 ms. The amplitudes of the correlation peaks were extracted from the 2D spectra to give the DQ curves presented in Figure S9. The DQ intensities were scaled with respect to the peak intensities in a 1D ^{29}Si CP MAS spectrum acquired with the same contact time of 40 ms and recycle delay of 2.5 s.

Table S7. NMR parameters for zeolite test sample **2**.

Peak	Chemical Shift[a] (ppm)	Relative Peak Area[a]	Peak Width at Half Height[a] (Hz)	% Lorentzian[a]	Correlated Peaks[b]
A	-113.1	2	26	83	A,B,C,E
B	-113.8	2	50	95	A,C,C,D
C	-116.8	2	40	73	A,B,B,D
D	-117.9	2	37	62	B,C,D,E
E	-118.5	1	35	82	A,A,D,D

[a] Obtained from deconvolution of 1D ^{29}Si CP MAS NMR spectrum (Figure S7). [b]Determined from the 2D ^{29}Si DQ correlation spectrum obtained with a recoupling time of 6 ms.

Table S8. Inter-site connectivity matrix* for zeolite test sample **2**.

	A	**B**	**C**	**D**	**E**
A	1	1	1	0	1
B	1	0	2	1	0
C	1	2	0	1	0
D	0	1	1	1	1
E	2	0	0	2	0

* The number in row *i* and column *j* indicates the number of Si sites *j* that are connected via Si-O-Si linkages to Si site *i.* Derived from the relative intensities of the correlation peaks in the 2D DQ correlation spectrum obtained with a recoupling time of 6 ms.

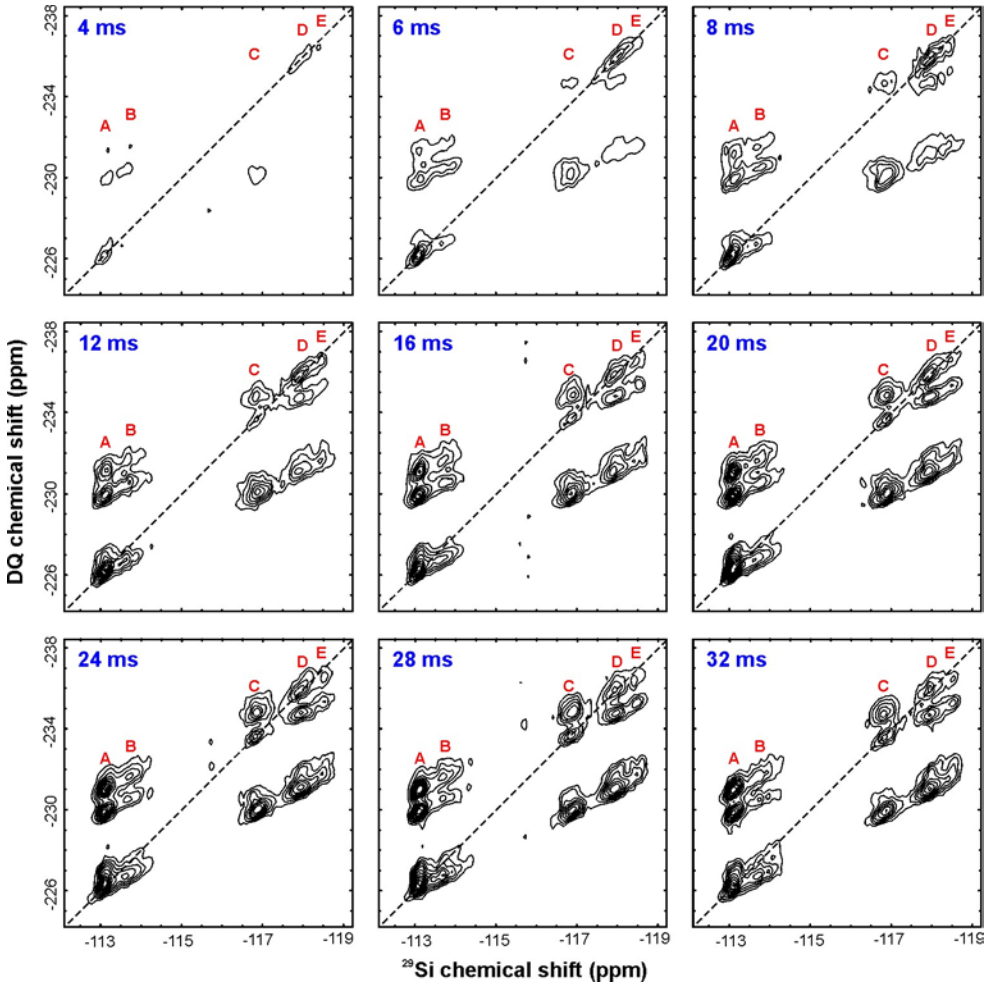

Figure S8. Two-dimensional ^{29}Si SR26$_4^{11}$ double-quantum correlation spectra of zeolite test sample **2** obtained at the indicated recoupling times.

5.4 Structure solution by solid-state NMR

The asymmetric unit for the *Pnnm* space group was chosen to be $0 \leq x < 1$, $0 \leq y \leq 1/4$, $0 \leq z < 1/2$. A three dimensional grid of the asymmetric unit was defined with a resolution of approximately 0.75 Å such that there were 10, 6, and 13 grid points in the *a*, *b*, and *c* directions respectively. By evaluating the "self-connectivity" information, the possible grid positions for sites A, B, C, D, and E were limited to 420, 484, 484, 420, and 484 positions respectively. The order in which the sites were added was set to {C,B,E,A,D}. Furthermore, the grid positions for the first site were

limited to those positions for which $0 \leq x \leq 1/4$ in order to cut down on the number of identical solutions which arise due to a number of equivalent choices of the origin. The number of grid structures at each stage of the grid search are presented in Table S9. The grid search required 1.5 hours of computation time.

Table S9. Summary of grid search for zeolite test sample **2**.

n	Added Si site	Possible positions for added Si site	New candidate structures	Consistent with relative occupancies	Consistent with inter-site connectivities	c_{select}	Best agreement with DQ curves*
1	C	143	143	143	143	1.5	93
2	B	484	44 919	27 965	4 138	1.4	112
3	E	484	53 984	11 424	6 062	1.3	586
4	A	420	245 898	210 884	19 184	1.2	2686
5	D	420	1 125 270	964 234	19 446	1.1	344

* Candidate structures with $R_{DQ} < c_{select}(R_{DQ})_{min}$ were selected

The 344 best grid structures were then subjected to non-linear least-squares minimization with the Si – Si distances across Si-O-Si linkages restrained to 3.10 ± 0.05 Å by setting $w_r = 0.18$. These minimized structures were compared to each other and 25 unique structures were identified. Oxygen atoms were added to each structure and the structures were subjected to DLS optimization in order to test the geometric feasibility of the structures. Additionally, the structures were evaluated for the presence of "three-rings" which are highly unlikely to be found in the structure, given the ^{29}Si chemical shifts observed. Only one of these structures gives a low R_{DLS} value (0.0063) and does not have any three-rings in the structure.

This "solid-state NMR structure" is presented in Figure 4 and the set of Si – Si distances calculated from this structure was used to calculate the DQ curves presented in Figure S9 (with R_{DQ} =

0.159, A = 1.86 and k = 32.0 s^{-1}). The structure obtained after adding the oxygen atoms and DLS optimization of the geometry was used for Rietveld refinement against the powder XRD data (see later). The solid-state NMR structure is compared to the refined structure in Figure 4e. The atomic coordinates for the Si sites determined by solid state are listed and compared to the to the refined coordinates in Table S11. The absolute differences in the atomic coordinates between the solid-state NMR and XRD-refined structure are all less than 0.7 Å. However, it should be noted that the structure obtained after adding the oxygen atoms and performing DLS brings the silicon positions to within 0.2 Å of the structure obtained after Rietveld refinement.

5.5 Structure refinement against powder XRD data

Structure refinement of zeolite test sample **2** was carried out using the whole pattern fitting (Rietveld) method incorporated into the GSAS suite of programs. The five silicon atoms from the NMR structure solution plus geometrically placed oxygen atoms (after subsequent DLS refinement) were used as the starting model, and the remaining carbon atoms of the organic templates were found from subsequent difference Fourier syntheses. This sample suffers from severe preferred orientation effects resulting from the plate-like habit of the crystals. The refinement after use of a March-Dollase preferred orientation correction required fairly strong soft constraints to maintain a chemically sensible geometry. The final cycle of least squares refinement included terms for the atomic positions of all the atoms, together with two variables for the silicon and oxygen isotropic displacement parameters respectively. The atoms of the templates were left unrefined. The final refinement cycle also included terms for the lattice parameters, diffractometers zero point and profile (peak shape and background). The refinement converged to values of R_p = 0.0639, wR_p = 0.0897. The observed, calculated and difference profiles for the refinement are shown in Figure S10. The final refined unit cell parameters and atomic coordinates are listed in Table S10.

Because of the difficulties with the preferred orientation in the powder data, the NMR-derived structure was also tested against single crystal X-ray diffraction data. While this data was collected on a slightly different, fluoride-containing sample of siliceous ferrierite[18] the silicon atom positions from

NMR were all that was necessary to successfully phase the data, and the oxygen atoms and the template atoms could be found from subsequent Fourier synthesis.

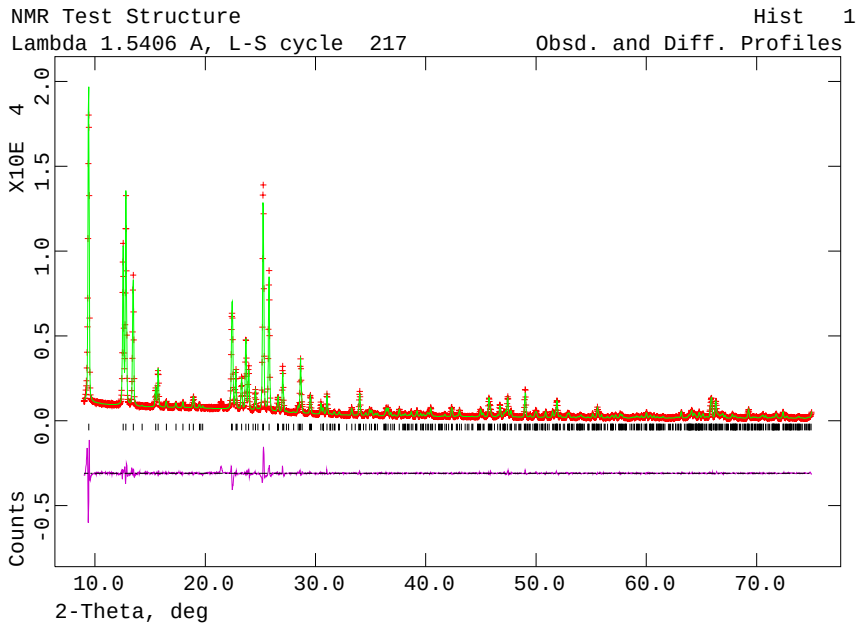

Figure S10. Rietveld refinement plot for zeolite test sample **2**. The observed (red crosses), calculated (green line) and difference (purple) plots for the Rietveld refinement of the structure against powder X-ray diffraction data.

Table S10. Final unit cell, refined coordinates and isotropic displacement parameters for zeolite test sample **2**.

Unit cell: a = 7.42899(20) Å, b = 14.0890(6) Å, c = 18.7440(8) Å Cell volume = 1961.87(12) Å^3

Atom	x	y	z	Uiso
Si1	0.2068(9)	-0.0060(8)	0.2251(4)	0.0131 (13)
Si2	0.7171(13)	0.2053(8)	0.1572(5)	0.0131 (13)
Si3	0.3104(13)	0.2092(9)	0.1824(5)	0.0131 (13)
Si4	0.5065(16)	0.2076(6)	0.4166(4)	0.0131 (13)
Si5	0.500000	0.000000	0.3557(7)	0.0131 (13)
O6	0.000000	0.000000	0.2518(11)	0.0325 (25)
O7	0.7268(30)	0.0914(10)	0.1717(12)	0.0325 (25)
O8	0.2470(28)	0.0994(10)	0.1914(12)	0.0325 (25)
O9	0.6669(18)	-0.0011(15)	0.2986(6)	0.0325 (25)
O10	0.5064(13)	0.2254(13)	0.1506(8)	0.0325 (25)
O11	0.7843(30)	0.2327(15)	0.2403(7)	0.0325 (25)
O12	0.8179(22)	0.2363(17)	0.0848(8)	0.0325 (25)
O13	0.6997(24)	0.2380(18)	0.3819(8)	0.0325 (25)
O14	0.5416(35)	0.2013(23)	0.500000	0.0325 (25)
O15	0.4853(35)	0.0953(7)	0.4026(8)	0.0325 (25)

Table S11. Comparison of Si fractional atomic coordinates for zeolite test sample **2** determined by solid-state NMR and subsequent refinement against powder XRD data.

Si site		Solid-state NMR	Powder XRD	Difference (Å)
A	*x*	0.2095	0.2068	0.40
	y	-0.0024	-0.0060	
	z	0.2041	0.2251	
B	*x*	0.6802	0.7171	0.30
	y	0.2124	0.2053	
	z	0.1616	0.1572	
C	*x*	0.2599	0.3104	0.41
	y	0.2187	0.2092	
	z	0.1777	0.1824	
D	*x*	0.4762	0.5065	0.51
	y	0.1751	0.2076	
	z	0.4178	0.4166	
E	*x*	0.5	0.5	0.66
	y	0	0	
	z	0.3202	0.3557	

5.6 Structure solution from powder XRD

All attempts to solve the structure of test sample **2** using Expo were unsuccessful. This is a much more challenging problem than the structure solution of test sample **1** because of the extra scattering of the occluded organic structure directing agents and the severe preferred orientation effects, which lead to unreliable intensity extraction from the XRD pattern. There are structure solution algorithms designed for use with samples of this kind[19] but this is a non-trivial problem and would still be extremely difficult.

---

1. Brouwer, D.H., Kristiansen P.E., Fyfe, C.A. & Levitt, M.H. Symmetry-based ^{29}Si dipolar recoupling magic angle spinning NMR spectroscopy: a new method for investigating three-dimensional structures of zeolite frameworks *J. Am. Chem. Soc.* **127**, 542-543 (2005).

2. Kristiansen, P. E., Carravetta, M., Lai, W. C. & Levitt, M. H. A robust pulse sequence for the determination of small homonuclear dipolar couplings in magic-angle spinning NMR. *Chem. Phys. Lett.* **390**, 1-7 (2004).

3. Carravetta, M., Eden, M., Zhao, X., Brinkmann, A. & Levitt, M. H. Symmetry principles for the design of radiofrequency pulse sequences in the nuclear magnetic resonance of rotating solids. *Chem. Phys. Lett.* **321**, 205-215 (2000).

4. Haeberlen, U. & Waugh, J.S. Coherent averaging effects in magnetic resonance. *Phys Rev.* **175**, 453-467 (1968).

5. Brinkmann, A. & Levitt, M. H. Symmetry principles in the nuclear magnetic resonance of spinning solids: Heteronuclear recoupling by generalized Hartmann-Hahn sequences. *J. Chem. Phys.* **115**, 357-384 (2001).

6. Gullion, T. & Schaefer, J. Rotational-echo double resonance NMR. *J. Magn. Reson.* **81**, 196-200 (1989).

7. Mueller, K. T. Analytic solutions for the time evolution of dipolar-dephasing NMR signals. *J. Magn. Reson. A* **113**, 81-93 (1995).

8. Mueller, K. T., Jarvie, T. P., Aurentz, D. J. & Roberts, B. W. The REDOR transform: direct calculation of internuclear couplings from dipolar-dephasing NMR data. *Chem. Phys. Lett.* **242**, 535-542 (1996).

9. Bak, M., Rasmussen, J. T. & Nielsen, N. C. SIMPSON: A General Simulation Program for Solid State NMR. *J. Magn. Reson.* **147**, 296-330 (2000).

10. Nocedal, J. & Wright, S.J. Numerical Optimization, Springer, New York (1999).

11. Baerlocher, Ch., Hepp, A. & Meier, W.M. DLS-76: a program for the simulation of crystal structures by geometric refinement. Lab. f. Kristallographie, ETH, Zurich (1978).

12. Baerlocher, Ch. & McCusker, L.B. Database of Zeolite Structures: http://www.iza-structure.org/databases/

13. Barrett, P.A, Camblor, M.A., Corma, A., Jones, R.H. & Villaescusa, L.A. Structure of ITQ-4, a new pure silica polymorph containing large pores and a large void volume *Chem. Mater.* **9**, 1713- 1715 (1997).

14. Werner, P.E., Eriksson, L. & Westdahl, M. *TREOR*, a semi-exhaustive trial-and-error powder indexing program for all symmetries *J. Appl. Crystallogr.* **18,** 367-370 (1985).

15. Larson, A.C., & Von Dreele, R.B. General Structure Analysis System (GSAS) Los Alamos National Laboratory Report LAUR 86-748 (2000).

16. Altomare, A. *et al*. EXPO: a program for full powder pattern decomposition and crystal structure solution, *J. Appl. Crystallogr.* **32**, 339-340 (1999).

17. Kuperman, A. *et al.* Nonaqueous synthesis of giant crystals of zeolites and molecular-sieves *Nature*, **365**, 239-242 (1993)

18. Bull, I. *et al*. An X-ray diffraction and MAS NMR study of the thermal expansion properties of calcined siliceous ferrierite, *J. Am. Chem. Soc.* **125**, 4342-4349 (2003)

19. McCusker, L.B. et al Solving complex zeolite structures from powder diffraction data *Chimia*, **55,** 497-504 (2001)